



# Characterization and electrochromic properties of NiO thin films prepared using a green aqueous solution by pulsed spray pyrolysis technique

M. Obaida<sup>1,a)</sup> , Ahlam M. Fathi<sup>2</sup>, I. Moussa<sup>1</sup>, H. H. Afify<sup>1</sup>

<sup>1</sup>Solid State Physics Department, Physics Research Institute, National Research Centre, 33 El Buhouth St., Dokki, Giza 12622, Egypt

<sup>2</sup>Physical Chemistry Department, National Research Centre, 33 El Buhouth St., Dokki, Giza 12622, Egypt

<sup>a)</sup>Address all correspondence to this author. e-mail: mohamed.obaida@rub.de

Received: 29 January 2022; accepted: 9 June 2022; published online: 28 June 2022

Nickel acetylacetonate of 0.2 M aqueous solution is used to synthesize (NiO) thin films by pulsed spray pyrolysis method onto glass substrates. Structural and morphological properties of the deposited films were examined using (XRD) and (FESEM) techniques. The results revealed that at low substrate temperatures and short spray time, the obtained films were amorphous, whereas the films deposited at higher temperatures and long spray time has a cubic phase. Cross-sectional FESEM is used to properly estimate films thicknesses. The energy band gap is calculated to be 3.52–3.89 eV using optical spectrum measurements. Electrochromic properties of NiO films deposited on FTO working electrode substrates are measured in a three-electrode cell containing KOH with Ag/AgCl reference electrode at a scan rate of 20 mV/s. The charge density increases with the thickness, and it is 98.0 mC/cm<sup>2</sup> at the thickness of 360 nm after 30-min deposition time at 400 °C and for most of the samples the film stability increases after cycling.

## Introduction

Spray pyrolysis technique is used for deposition n-type transparent conductive oxides such as zinc oxide (ZnO) and indium-tin oxide (ITO) which are widely used for solar cell electrodes, window coatings, etc. [1]. However, new p-type transparent conducting thin films are prepared for useful versatile applications such as fabrication of dye-sensitized solar cells, chemical sensors, smart windows (ultraviolet, visible or (near) infrared radiation block) for saving energy consumption [2–9]. Electrochromic phenomenon means change in material transmission to nearly opaque by reverse the polarity of low applied potential 1.5 V. It is very useful in solar radiation spectrum control. Buildings and vehicle glass windows coated with an electrochromic film reduce the entered solar radiation thereby the internal temperature will be minimized. Based upon the windows coated with heat mirror fabricated by spray pyrolysis technique will reduce the consumed energy for cooling appliances; nickel oxide is a prominent in electrochromic family material. Nickel oxide films have various properties due to their high electrochromic efficiency, including cyclic reversibility (very stable), endurance, and color [10]. Nickel

oxide (NiO) has excellent chemical stability and wide band gap of 3.0–4.3 eV is considered as one of the best examples of p-type semiconductor metal oxide thin films [11–15]. The conductivity in p-type semiconductor materials is usually related to the excess of oxygen atoms or due to the lack of metal atoms compound in their forming structure [16]. Moreover, due to NiO electronic band structure, robust durability, electrochromic efficiency, and cyclic reversibility all make it valuable and promising for different modern applications such as smart windows technology.

Many of chemical and physical deposition techniques have been used to synthesis NiO thin films such as sol–gel, sputtering, pulsed spray pyrolysis, spin coating, and pulsed laser deposition [17–21]. Among these techniques pulsed spray pyrolysis (PSP) has many advantageous such as low cost, easy to operation, no vacuum, produce multi-state film (amorphous, crystalline, porous, compact, excellent adherence) with the ability for mass production of films with wide area [21]. The main advantage of this system is keeping the substrate temperature constant all over the spray process which is a main problem in pneumatic spray systems. The properties of the produced film depend mainly on

molarity of the precursors, substrate temperatures, substrate to nozzle distance, spray time, and gas carrier flow rate. The mostly used precursors to prepare NiO are nitrates and chlorides which need more precautions due to its hazards. Herein, nickel Acetylacetonate is used as safe and benign precursor for synthesis of an electrochromic NiO film.

This manuscript is devoted to exploring at what extent the quality of the deposited NiO film on bare and FTO-coated glass substrates by the LAB team homemade and assembled PSP system using green spray solution via its characterization. Structural, optical, and electrochromic properties are appointed by XRD, FESEM, optical transmission, and cyclic voltammetry. The obtained results not only support a simple, easy, and safety technique but also enrich the data related to electrochromic phenomenon of NiO films. The preparation and characterization of NiO films could be considered valuable, since up to date no studies have been done using nickel acetylacetonate as a precursor in the form of aqueous solution [12]. The electrochromic (EC) properties of the prepared NiO films from nickel acetylacetonate precursor at both different deposition temperatures and spray time will be investigated in the light of structural, morphological, and optical results of the synthesized films to determine the optimum preparation conditions giving rise to produce an electrochromic film with high performance of shorter response time and high reversibility from transparency to dim nature at lower applied voltage.

## Results and discussion

### XRD characterization

The X-ray diffraction patterns of the deposited films at both different temperatures and spray times are shown in Fig. 1(a, b). The deposited films are polycrystalline; all the diffraction peaks (111), (200), (220), (311), (222) are indexed with JCPDS files and it is matched with the data sheet No. (# 00-065-2901) corresponding to NiO with cubic phase and space group [Fm-3m (225)]. No other phases or crystalline impurities are detected, indicating the phase singularity of the synthesized NiO thin films.

The lattice parameter  $a$  is calculated by  $a = d \times \sqrt{h^2 + k^2 + l^2}$   $a = d \times \sqrt{h^2 + k^2 + l^2}$ , where  $(hkl)$  are the Miller indices and  $(d)$  is the interplanar spacing given by  $2d_{hkl} \sin(\theta_{hkl}) = \lambda$ ,  $\theta_{hkl}$  is Bragg's angle,  $\lambda$  is the wavelength of X-ray. In Table 1, the crystallite size  $D$  and strain  $\epsilon$  values for all the samples are calculated (from the slope and the cutting part from the  $y$ -axis of the plot) using Williamson–Hall Plot defined  $\beta_{hkl} \cos \theta_{hkl} = (k\lambda/D) + 4\epsilon \sin \theta_{hkl}$  [22], since  $\beta_{hkl}$  is the broadening (FWHM) of the peak. The obtained results show that the

deposited films are polycrystalline due to the existence of more than one plane of growth with a nanosized scale because of lower intensity of peaks. An observable increase in both lattice parameter and crystallite size is induced by increasing deposition temperature and spray time, whereas the strain decreases. This could be interpreted as some sort of relaxation resulting in lattice when both deposition time and temperature are increased which allows an increase and decrease in crystallite size and internal strain, respectively.

### SEM

Field Emission Scanning Electron Microscope FESEM is used to investigate the surface morphological structure of the deposited NiO films. The obtained images for the examined sample NO2, NO5, NO7, NO8, and NO9 are displayed in Fig. 2(a–e). Nearly individual round small particles are found in neighbor with some large cluster embrace, where some of them indicating some sort of surface roughness of NO2 sample marked by both deposition temperature 400 °C & time 30 min are observed in Fig. 2(a). The protruding surface roughness may be due to that the growth process is fast inducing small crystallites conjugated with some clusters.

The limiting factors temperature and time for diffusing process are not sufficient to make complete diffusion of the composed microstructures allowing lower level of roughness. This is supported by the decrease in surface roughness level by the increase in temperature or time or both as observed in Fig. 2(a, d) of samples deposited at 400 & 500 °C. The improvement in surface homogeneity is found as the deposition temperature rises to 450 and 500 °C as shown in Fig. 2(b, c) at spray time of 30 min. The crystalline quality of the deposited films is increased which synergies with the decrease in broadening and increase in intensity of peaks recorded in XRD patterns. The surface morphologies of the films NO7, NO8, and NO9 deposited at different spray times (10, 30, 50 min) and constant substrate temperature of 500 °C are shown in Fig. 2(c–e).

For NO7 and NO8 samples, a well-closed surface structure with an interconnected grains and compact morphology is found, indicating good adhesion to the substrate surface without micro cracks or pinholes as shown in Fig. 2(c, d). In contrast as shown in Fig. 2(e), sample NO9 has formed agglomerates which may be attributed to the long spray time. EDX spectra revealed the presence of Ni and O atoms in the synthesized films. The thickness of the investigated samples is estimated from the cross-sectional FESEM images [21]. The recorded thicknesses for NO2, NO5, NO7, NO8, and NO9 films are 360, 327, 192, 233, and 403 nm, respectively.

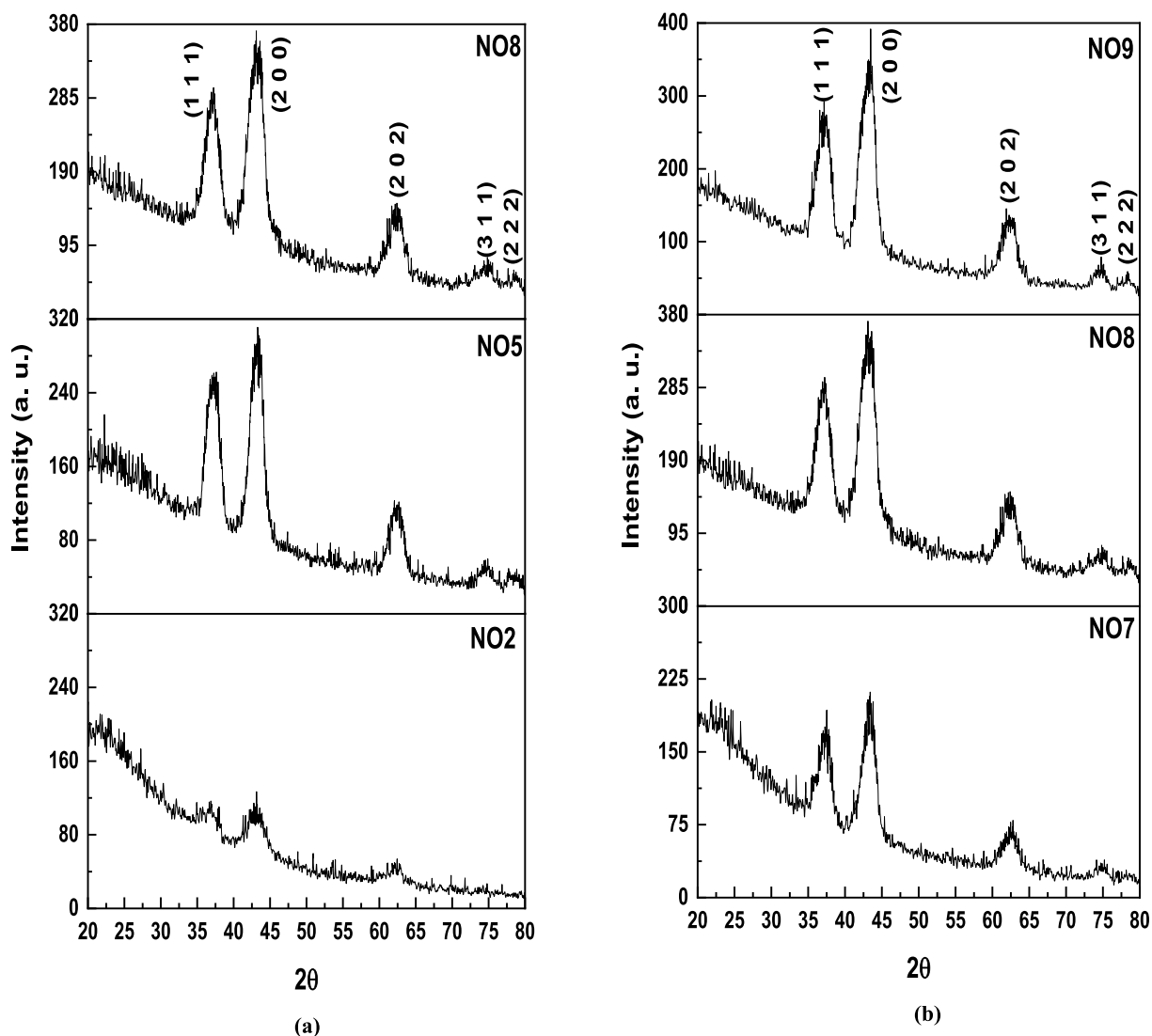


**Figure 1:** XRD charts of the spray deposited NiO films, (a) XRD patterns of films deposited for constant 30 min at 400 °C (NO2), 450 °C (NO5), and 500 °C (NO8), (b) XRD patterns of films deposited for at constant 500 °C for 10 (NO7), 30 (NO8), and 50 (NO9) minutes.

**TABLE 1:** The calculated Crystallographic information for the deposited films.

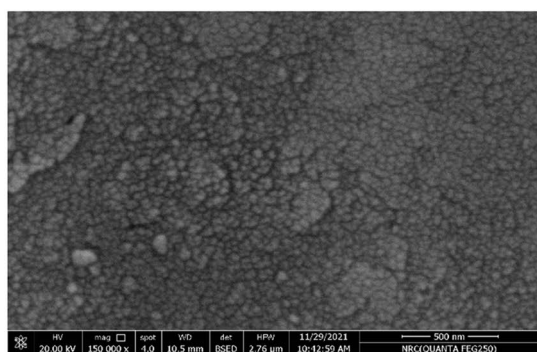
Sample	Crystallographic information		
	Lattice parameter $a$ , (Å)	Crystallite size $D$ , (nm)	Strain ( $\epsilon$ )
NO2 (400 °C, 30 min)	4.15	3.18	0.006
NO5 (450 °C, 30 min)	4.17	3.68	0.005
NO7 (500 °C, 10 min)	4.18	4.22	0.002
NO8 (500 °C, 30 min)	4.19	4.49	0.002
NO9 (500 °C, 50 min)	4.20	5.50	0.001

### Optical measurements

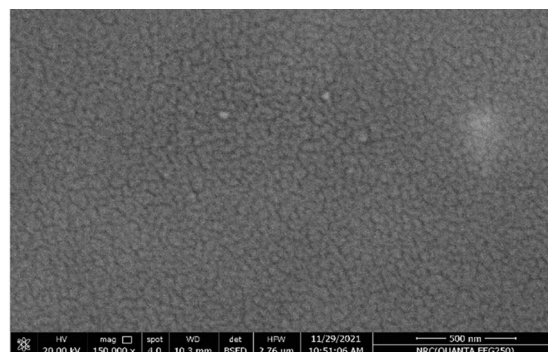
Nickel oxide thin films have a fascinating optical switching property. High transparency of NiO film is reversibly converted

to nearly opaque when a lower potential (about 1 V) is applied. Such material is promising for a wide range of electrochromic applications especially solar spectrum modulation. To provide a comprehensive insight, the optical Transmittance ( $T$ ) & Reflectance ( $R$ ) spectra are measured for NiO films when subjected to lower potential in an electrolyte by a spectrophotometer provided with a special measuring cell.

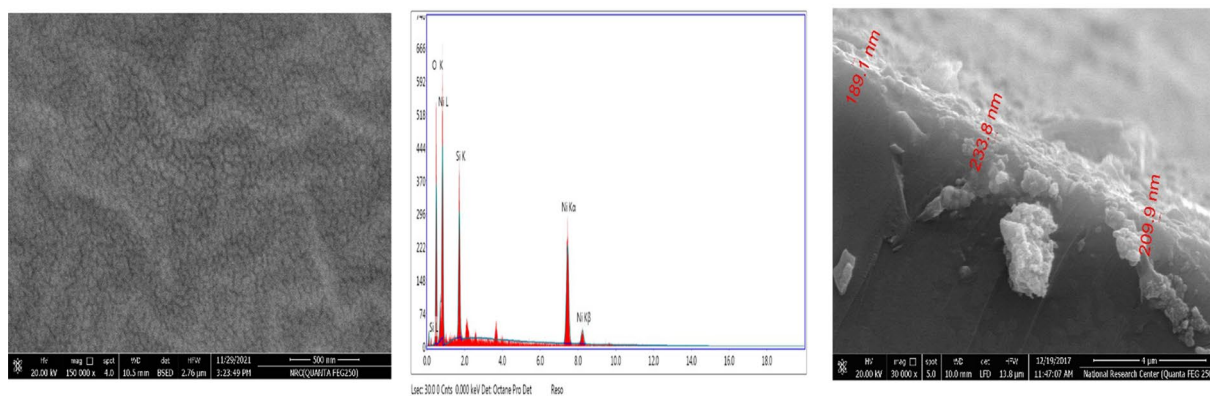
The LAB facilities for performing these measurements are not available. Therefore, the typical transmission and reflection measurements are carried out by a normal double-beam spectrophotometer without immersing the samples in an electrolyte and potential application. Therefore, optical switching as an electrochromic phenomenon is measured by the well-known cyclic voltammetry technique. The typical measurements of T&R for the NiO film samples (group A) prepared at constant substrate



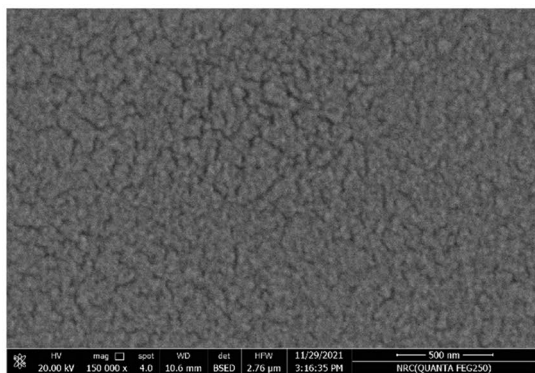
(a) Sample NO2 (400°C-30 minutes)



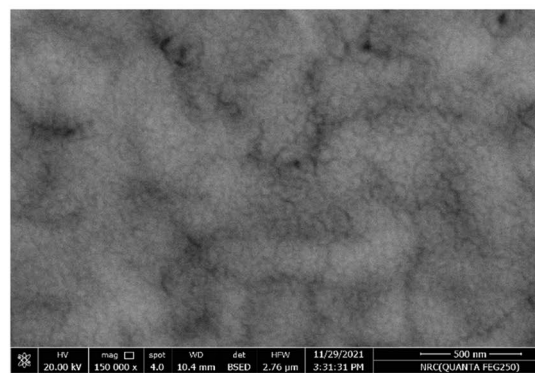
(b) Sample NO5 (450°C-30 minutes)



(c) Sample NO8 (500°C-30 minutes) SEM, EDX and Cross section images.



(d) Sample NO7 (500°C-10 minutes)



(e) Sample NO9 (500°C-50 minutes)

Figure 2: FESEM images for NiO films deposited at different temperatures and spray times.

temperature 500 °C and variable spray time 10, 30, and 50 min and those (group B) deposited at constant spray time 30 min and varied substrate temperatures 400, 450, and 500 °C are executed.

The spectrum curve for each sample is demonstrated in Fig. 3. The most salient feature is all samples show high transmittance (nearly 90 to 70%) and round spectrum curves. Also, the sharp absorption edge is not observed which means that the energy gap is not empty, but it contains non-intentional impurity levels and non-stoichiometry level such as oxygen vacancies

or excess Nickel. It is clear that samples of group (A) exhibit reasonable decrease in transmission conjugated with the increase in deposition time.

This observation is mainly related to the increase in film thickness and the induced film compactness as supported by FESEM images and the measured values of film thickness. Also, thicker films have lower transmittance due to the existence of larger crystallite sizes, bigger clusters as well as higher surface roughness which increase light scattering. On the





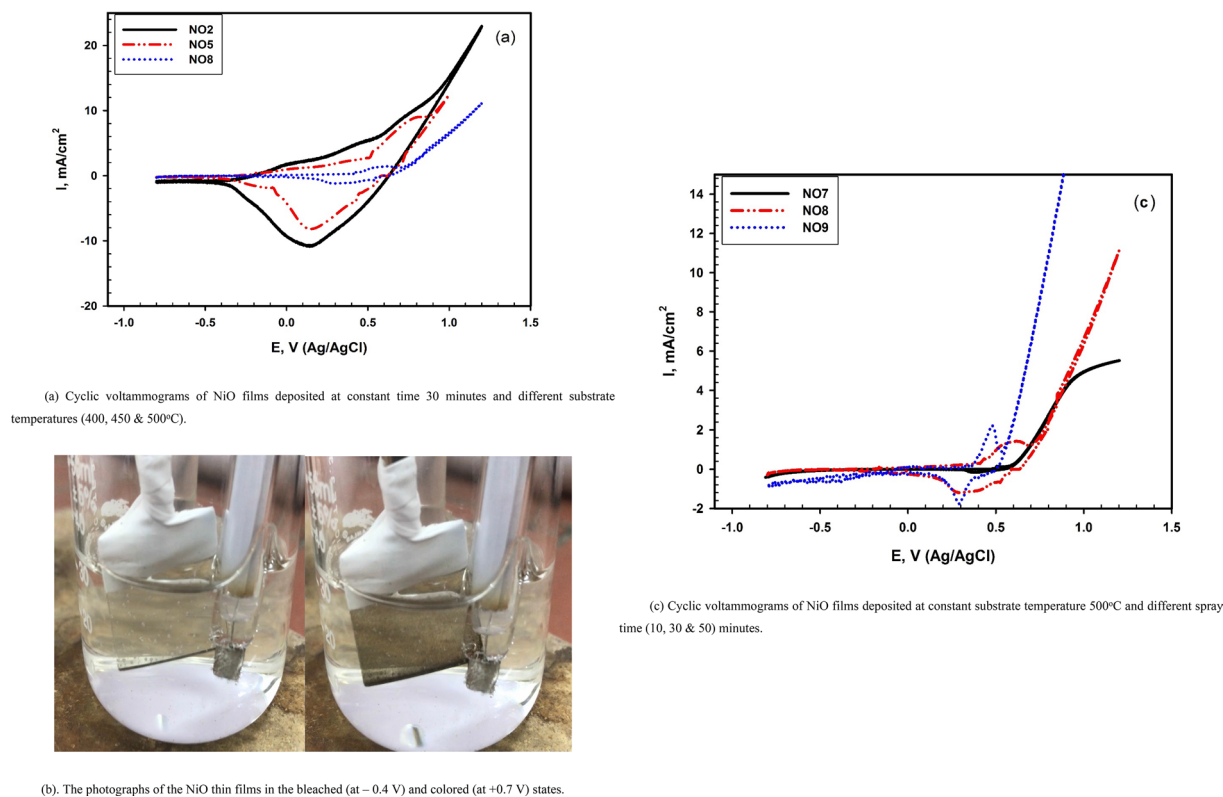


**Figure 5:** (a) Cyclic voltammograms of NiO films deposited at constant time 30 min and different substrate temperatures (400, 450, & 500 °C). (b) The photographs of the NiO thin films in the bleached (at -0.4 V) and colored (at +0.7 V) states. (c) Cyclic voltammograms of NiO films deposited at constant substrate temperature 500 °C and different spray times (10, 30, & 50) min.

**TABLE 2:** Determination of the amount of the charge intercalated into and out of the film ( $q_a$  &  $q_c$ ),  $\Delta q$  ratio, and the charge density ( $Q$ ).

Name	NO2	NO5	NO7	NO8	NO9
$q_a$ (mC)	5.97	2.61	0.04	0.22	0.36
$q_b$ (mC)	6.33	3.48	0.05	0.20	0.38
$\Delta q$	1.06	1.30	1.25	0.91	1.05
$Q$ (mC/cm <sup>2</sup> )	98.0	58.56	0.77	4.04	7.0

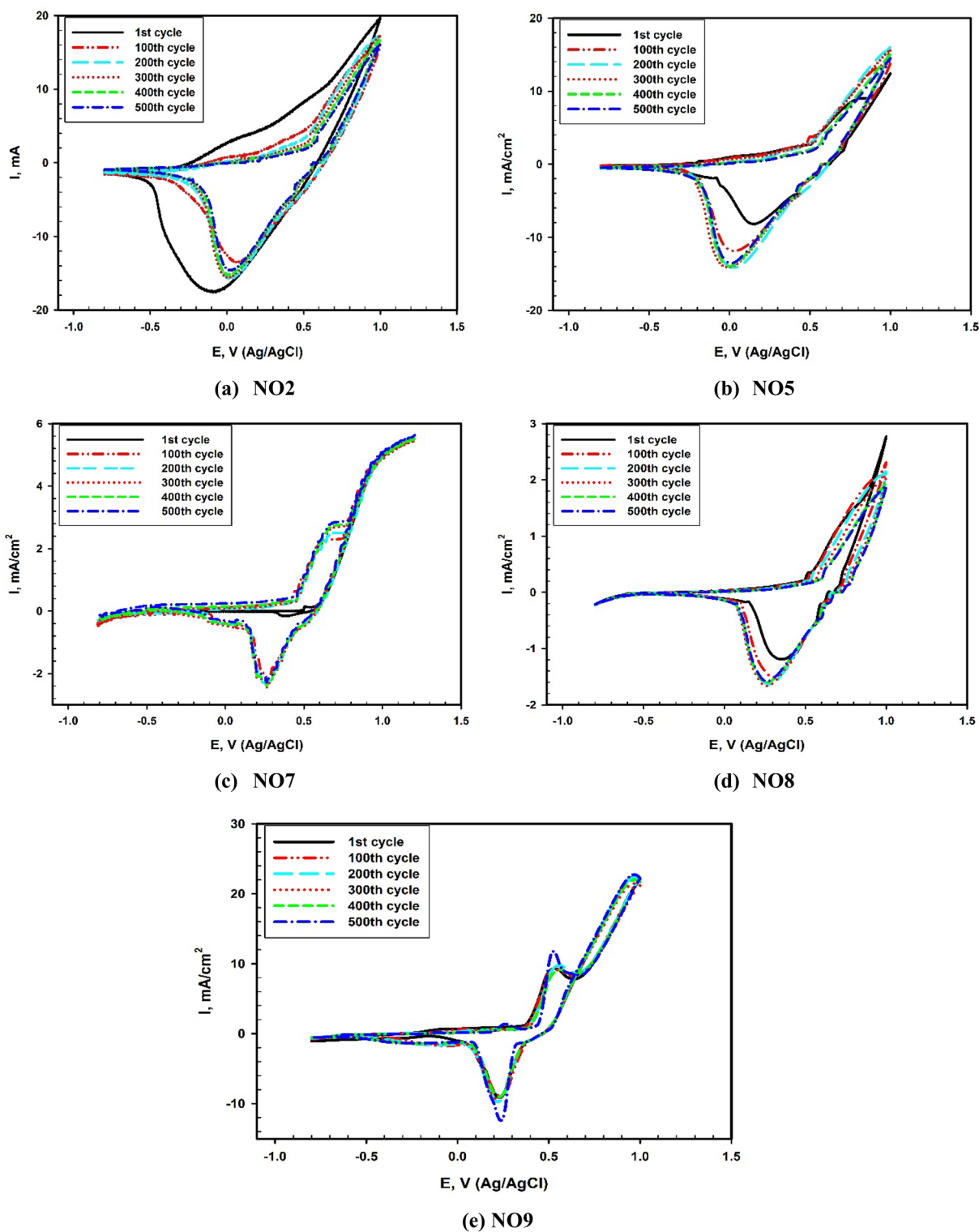
The amount of the charge intercalated out ( $q$  anodic) and into ( $q$  cathodic) of the film ( $q_a$  &  $q_c$ ) during the redox reaction is calculated by the integration of the anodic and cathodic area separately for the three samples. The obtained values are listed in Table 2. The ratio  $\Delta q$  is calculated ( $\Delta q = q_c/q_a$ ) and listed in Table 2 where the values near one indicate the reversibility of the redox process, which suggests that NiO films have a good reversibility in 0.1 M KOH electrolyte [24]. The samples NO2 and NO9 fulfill the reversibility of charge intercalation. The charge density ( $Q$ ) of the NO2, NO5, NO7, NO8, and NO9 films calculated from the CV curve at scan rate of 0.02 V/s according to the following relation [31] is found to be 98.0, 58.56, 0.77, 4.04, and 7.0 mC/cm<sup>2</sup> respectively.

$$Q = \frac{1}{\nu A} \int_{V_i}^{V_f} I dV, \quad (1)$$

where  $\nu$  is the scan rate,  $V_i$  is the initial scanned potential,  $V_f$  is the final scanned potential,  $I$  is the current, and  $A$  is the area of the working electrode surface. To investigate the redox stability of the film in 0.1 M KOH, the cyclic voltammetry was repeated for 500 cycles at scan rate 0.1 V/s as shown in Fig. 6(a-e).

It is fascinating to show good redox stability after 500 oxidation-reduction cycles where the peak current reduced to nearly 50% of the peak current of the first cycle for NO2 sample which may be due to the detachment of the film from FTO surface [3, 32] or may be due to the irreversible intercalation of the hydroxyl group to the oxide film [32]. However, the peak current after 100-500 cycles increased to more than twofold of the peak current of the first cycle for samples NO5, NO7, NO8, and NO9 indicating the increase in the stability of the redox reaction with time which suggests modification in the nature and morphology of the film during cycling [32].

This behavior is happened when a porous film is used and due to that not all the possible surface area was



The cyclic voltammety measurements at different number of scanning cycles.

**Figure 6:** (a–e) The cyclic voltammety measurements at different number of scanning cycles.

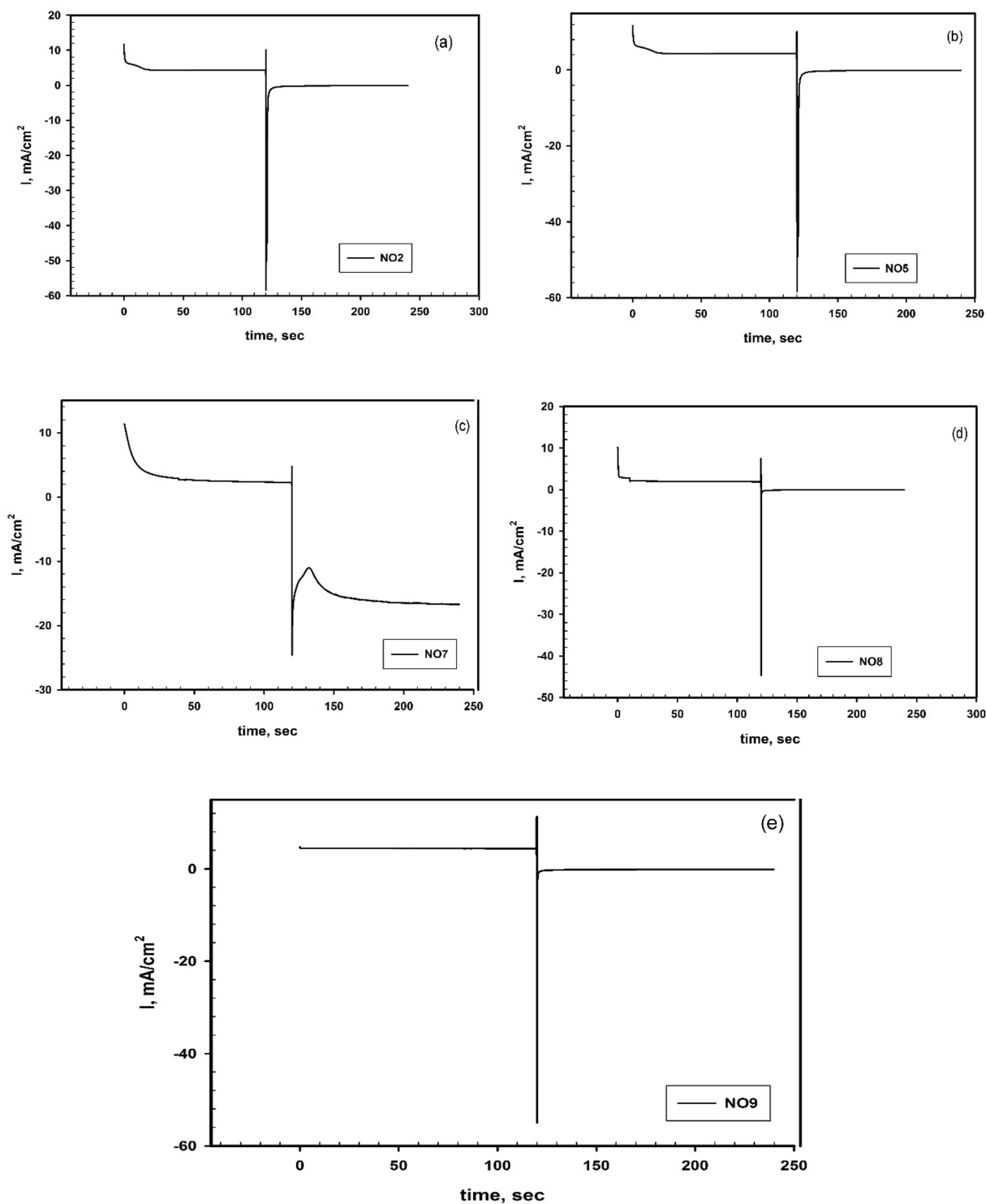


**Figure 7:** (a–e) The recorded speed of the redox reaction of the deposited NiO thin films.

accessible to the electrolyte at the start of the experiment. But with cycling, all the sites become accessible where the intercalation of OH ions in the pores establish an electronic connectivity throughout the deposited film [3, 32]. In addition, a shift of the oxidation to higher values and the

reduction peaks to lower values result in the increase in the peak separation. To determine the speed of the redox reaction, chronoamperometry (CA) technique was performed for the samples in the potential range from  $-0.7$  to  $0.7$  V (Ag/AgCl) as shown in Fig. 7(a–e).



It was noted that the current decreases with time due to the increase in the chemical potential of the intercalated ions. The response time for the coloration ( $t_c$ ) and discoloration ( $t_d$ ), which are the time needed for anodic and cathodic current to reach a steady state after applying certain potential, are very essential to study the performance of the electrochromic devices. After applying 0.7 V, the anodic current for NO2, NO5, NO7, NO8, and NO9 decreases to reach a steady state of about 5.0, 4.5, 3, 2.8, and 4.7 mA/cm<sup>2</sup> within 4, 16, 18, 6, and 0.1 s, respectively, while on switching to the negative potential – 0.7 V, the current decreases to attain steady state at 0.03, – 0.17, – 15.4, 0.28, and – 0.39 mA/cm<sup>2</sup> within 1.5, 5, 19, 2, and 1.5 s, respectively. The values of  $t_c$  and  $t_d$  obtained for NO9F are better than the values obtained in different previous works [27, 32, 33]. The response time was dependent on several factors such as applied potential, thickness of the films, and electrolyte conductivity [34].

## Conclusion

At different deposition temperatures and spray times an electrochromic dopant-free NiO film is prepared successfully on glass substrates by PSP system, and the following conclusions were reached from the findings:

- At high deposition temperatures, NiO films are polycrystalline with a cubic phase and nanosized scale, according to XRD analysis. At low deposition temperature and long spray time, FESEM micrographs revealed a rough film surface, and the existence of Ni and O atoms was revealed by EDX spectra.
- The measured optical spectra curves stated clearly strong transmittance of 85% with a predicted band gap ranging from 3.52 to 3.89 eV.
- Electrochromic (EC) characteristics of NiO thin films deposited on FTO substrates showed that the samples prepared at highly deposition temperatures and long spray times of 500 °C (30 and 50 min) fulfill the reversibility of charge intercalation condition during dim and bleaching electrochromic behavior, and the best recorded values for  $t_c$  and  $t_d$  values were found in samples deposited at 500 °C and 50 min. Based on these obtained results, the prepared NiO thin films could be considered as a promising candidate to reduce the consumed energy required for cooling appliances.

## Materials and methods

### Preparation of NiO thin films

Anhydrous nickel (II) acetylacetonate (C<sub>10</sub>H<sub>14</sub>NiO<sub>4</sub>) with a concentration of 0.2 M dissolved in 95 ml of distilled water and 5 ml acetic acid stirred vigorously at 40 °C for 15 min are

used as a precursor solution for deposition of nickel oxide thin films. Pulsed spray pyrolysis (PSP) system is used to prepare the synthesized films at different temperatures and varied deposition time [NO2 (400 °C, 30 min), NO5 (450 °C, 30 min), NO7 (500 °C, 10 min, NO8 (500 °C, 30 min), and NO9 (500 °C, 50 min)] on ultrasonically and chemically cleaned glass substrates. To keep the temperature, stable at the substrate surface, the aerosol solution is intermittent through interval of (1 s for ON and 4 s for Off mode).

All other spraying parameters such as gas (air) carrier flow rate of 25 cm<sup>3</sup>/min, atomizer to substrate distance maintained at 30 cm. Solution deposition interval and molarities are kept constant to obtain uniform, homogeneous, and well-adhered films on the surface of the glass substrate. The applied procedure to great extent is different by its safety and simplicity than those used in published papers.

### Characterization of NiO thin films

X-ray diffractometer (XRD) Empyrean from PANalytical Netherland is used to record the XRD patterns for the investigated samples to elucidate the existed phases and crystal nature of the deposited films in the scan range 2θ from 10° to 80°. The surface morphology of the synthesized thin films is examined using field emission scanning electron microscope (FESEM-Quanta FEG 250 with field emission gun, FEI company-Netherland) and the energy-dispersive X-ray spectroscopy (EDX) is also used to provide elemental identification of the prepared films. The thickness of the samples is determined from the cross-sectional FESEM images. Optical properties measurements are performed using UV–Vis–NIR double-beam spectrophotometer (Jasco-750 V) within a wavelength from 0.3 to 2.5 μm. The optical band gap ( $E_g$ ) of NiO films is determined using Tauc's extrapolation plot [23].

### Electrochromic measurements

Electrochromic investigations are carried out in a three-electrode conventional glass cell in 0.1 M KOH solution at 25 °C using Orignalys OGS 200 potentiostat/galvanostat. The potential of the working electrode will be measured against Ag/AgCl reference electrode ( $E_o = 0.203$  V vs. SHE) and pure Pt sheet will be used as counter electrode. The working electrode is prepared as a NiO thin film on transparent conductive glass substrates coated with FTO. Cyclic voltammetry curves are used to characterize the electrochemical behavior of electrodes at 20 and 100 mV/s sweep rates covering a potential range between – 0.8 and 1.0 V (vs. Ag/AgCl) after 5 min of immersion in electrolyte (25 °C). The chronoamperometry (CA) measurements are evaluated at a potentials range of – 0.7 and + 0.7 V.

## Funding

Open access funding provided by The Science, Technology & Innovation Funding Authority (STDF) in cooperation with The Egyptian Knowledge Bank (EKB).

## Data availability

The authors confirm that the data supporting the findings of this study are available within the article and its supplementary materials.

## Declarations

**Conflict of interest** The authors declare that there are no conflict of interest.

## Open Access

This article is licensed under a Creative Commons Attribution 4.0 International License, which permits use, sharing, adaptation, distribution and reproduction in any medium or format, as long as you give appropriate credit to the original author(s) and the source, provide a link to the Creative Commons licence, and indicate if changes were made. The images or other third party material in this article are included in the article's Creative Commons licence, unless indicated otherwise in a credit line to the material. If material is not included in the article's Creative Commons licence and your intended use is not permitted by statutory regulation or exceeds the permitted use, you will need to obtain permission directly from the copyright holder. To view a copy of this licence, visit <http://creativecommons.org/licenses/by/4.0/>.

## References

1. A.J.M. Stadler, Transparent conducting oxides—an up-to-date overview. *Materials* **5**(4), 661–683 (2012)
2. J. Ahmad, K. Majid, M.A.J.A.S.S. Dar, Controlled synthesis of p-type NiO/n-type GO nanocomposite with enhanced photocatalytic activity and study of temperature effect on the photocatalytic activity of the nanocomposite. *Appl. Surf. Sci.* **457**, 417–426 (2018)
3. M.P. Browne et al., Electrochromic nickel oxide films for smart window applications. *Int. J. Electrochem. Sci* **11**, 6636–6647 (2016)
4. M. Fouladgar, S.J.A.S.S. Ahmadzadeh, Application of a nanostructured sensor based on NiO nanoparticles modified carbon paste electrode for determination of methyl dopa in the presence of folic acid. *Appl. Surf. Sci.* **379**, 150–155 (2016)
5. C. Huang et al., Synthesis of polyaniline/nickel oxide/sulfonated graphene ternary composite for all-solid-state asymmetric supercapacitor. *Appl. Surf. Sci.* **505**, 144589 (2020)
6. R.S. Kate, S.C. Bulakhe, R.J. Deokate, Effect of substrate temperature on properties of nickel oxide (NiO) thin films by spray pyrolysis. *J. Electron. Mater.* **48**(5), 3220–3228 (2019)
7. P. Lv et al., Self-assembled three-dimensional hierarchical NiO nano/microspheres as high-performance anode material for lithium ion batteries. *Appl. Surf. Sci.* **329**, 301–305 (2015)
8. W. Maiaugree et al., Efficiency enhancement for dye-sensitized solar cells with a porous NiO/Pt counter electrode. *Appl. Surf. Sci.* **289**, 72–76 (2014)
9. U.T. Nakate et al., Ultra thin NiO nanosheets for high performance hydrogen gas sensor device. *Appl. Surf. Sci.* **506**, 144971 (2020)
10. F. Ferreira et al., Electrochromic nickel oxide thin films deposited under different sputtering conditions. *Solid State Ionics* **86**, 971–976 (1996)
11. J. Desai et al., Spray pyrolytic synthesis of large area NiOx thin films from aqueous nickel acetate solutions. *Appl. Surf. Sci.* **253**(4), 1781–1786 (2006)
12. N. Kumar et al., Large-area, green solvent spray deposited nickel oxide films for scalable fabrication of triple-cation perovskite solar cells. *J. Mater. Chem. A* **8**(6), 3357–3368 (2020)
13. P. Patil, L.J.A.S.S. Kadam, Preparation and characterization of spray pyrolyzed nickel oxide (NiO) thin films. *Appl. Surf. Sci.* **199**(1–4), 211–221 (2002)
14. J. Sun et al., Piezo-phototronic effect enhanced photo-detector based on ZnO nano-arrays/NiO structure. *Appl. Surf. Sci.* **427**, 613–619 (2018)
15. K. Ukoba et al., Review of nanostructured NiO thin film deposition using the spray pyrolysis technique. *Renew. Sustain. Energy Rev.* **82**, 2900–2915 (2018)
16. A. Janotti, C.G. Van de Walle, Fundamentals of zinc oxide as a semiconductor. *Progr. Phys.* **72**(12), 126501 (2009)
17. J. Keraudy et al., Nitrogen doping on NiO by reactive magnetron sputtering: A new pathway to dynamically tune the optical and electrical properties. *Appl. Surf. Sci.* **409**, 77–84 (2017)
18. Y.-M. Lee, C.-H. Hsu, H.-W.J.A.S.S. Chen, Structural, optical, and electrical properties of p-type NiO films and composite TiO<sub>2</sub>/NiO electrodes for solid-state dye-sensitized solar cells. *Appl. Surf. Sci.* **255**(8), 4658–4663 (2009)
19. Q. Xi et al., Highly efficient inverted perovskite solar cells mediated by electrodeposition-processed NiO NPs hole-selective contact with different energy structure and surface property. *Appl. Surf. Sci.* **463**, 1107–1116 (2019)
20. H. Yang et al., Improved electrochromic properties of nanoporous NiO film by NiO flake with thickness controlled by aluminum. *Appl. Surf. Sci.* **461**, 88–92 (2018)

21. M. Obaida et al., Enhancement of photocatalytic activity for nanostructured ZnO thin film prepared by pulsed spray pyrolysis. *Egypt. J. Chem.* **63**(6), 2331–2344 (2020)
22. G. Williamson, W.J.A. Hall, X-ray line broadening from filed aluminium and wolfram. *Acta Metall.* **1**(1), 22–31 (1953)
23. J. Tauc, R. Grigorovici, A. Vancu, Optical properties and electronic structure of amorphous germanium. *Phys. Status Solidi B* **15**(2), 627–637 (1966)
24. L. Kadam, P.S. Patil, Studies on electrochromic properties of nickel oxide thin films prepared by spray pyrolysis technique. *Solar Energy Mater. Solar Cells* **69**(4), 361–369 (2001)
25. I. Bouessay, A. Rougier, J.-M. Tarascon, Electrochemically inactive nickel oxide as electrochromic material. *J. Electrochem. Soc.* **151**(6), H145 (2004)
26. A.M. Fathi, H.T. Handal, A.A.J.C.L. El-Kady, Rice straw derived activated carbon-based Ni-containing electrocatalyst for methanol oxidation. *Carbon Lett.* **31**(2), 253–267 (2021)
27. A.C. Nwanya et al., Electrochromic and electrochemical supercapacitive properties of room temperature PVP capped Ni (OH) <sub>2</sub>/NiO thin films. *Electrochim. Acta* **171**, 128–141 (2015)
28. A. Agrawal et al., Effect of deposition pressure on the microstructure and electrochromic properties of electron-beam-evaporated nickel oxide films. *Thin Solid Films* **221**(1–2), 239–253 (1992)
29. J. Nagai, Characterization of evaporated nickel oxide and its application to electrochromic glazing. *Solar Energy Mater. Solar Cells* **31**(2), 291–299 (1993)
30. M. Uplane et al., Structural, optical and electrochromic properties of nickel oxide thin films grown from electrodeposited nickel sulphide. *Appl. Surf. Sci.* **253**(24), 9365–9371 (2007)
31. E. Kalu et al., Cyclic voltammetric studies of the effects of time and temperature on the capacitance of electrochemically deposited nickel hydroxide. *J. Power Sources* **92**(1–2), 163–167 (2001)
32. X. Xia et al., Electrochromic properties of porous NiO thin films prepared by a chemical bath deposition. *Sol. Energy Mater. Sol. Cells* **92**(6), 628–633 (2008)
33. D. Dalavi et al., Nanoporous nickel oxide thin films and its improved electrochromic performance: Effect of thickness. *Appl. Surf. Sci.* **257**(7), 2647–2656 (2011)
34. M. Fantini, A.J.S.E.M. Gorenstein, Electrochromic nickel hydroxide films on transparent/conducting substrates. *Solar Energy Mater. Solar Cells.* **16**(6), 487–500 (1987)